# Dynamic and Quasi-Static Mechanical Response and Associated Microstructural Evolution of Damascus Steels

**A. M. W. Wackwitz, A. A. H. Ameri, J. Wang, P. Hazell, H. Wang, H. Timmers, and J. P. Escobedo-Diaz**

**Abstract**   This study examines the mechanical response and microstructural evolution of modern manufactured high carbon pattern welded Damascus steels. The characterisation consists of quasi-static and dynamic compression testing, optical microscopy, ultrasonic sound speed measurements, and Vickers hardness. The results from the quasi-static compression testing at a strain rate of $10^{-3}$/s show that the yield strength of the materials is approximately 500 MPa, which is comparable to that of plain carbon steel (~450 MPa) and display similar strain hardening properties. The compression results also display a slightly higher Young's Modulus for samples with layer orientation perpendicular to the uniaxial load than those with layer orientation of approximately 45° to the uniaxial load. Dynamic testing using a Split-Hopkinson Bar results showed a similar yield strength of ~ 1150 MPa for the samples with 45° layer orientation, whereas samples with perpendicular orientation showed a slight increase in the yield stress with increasing the strain rate.

**Keywords**  Iron and steel · Mechanical properties · Characterization

## Introduction

Damascus steel has long held a reverence because of its excellent performance characteristics and has been shrouded in mystery since its discovery by Europeans. A contributing factor to this has been the controversial and conflicting literature published based on the origins of the steel. The performance of Damascus steel, or Wootz steel, is entwined with the history of the steel and the legends of its performance [1]. This fame caused the spread of Damascus steel through the Middle East after the Christian Crusades. Due to the somewhat legendary status of this steel,

A. M. W. Wackwitz (✉) · A. A. H. Ameri · J. Wang · P. Hazell · H. Wang · H. Timmers · J. P. Escobedo-Diaz
University of New South Wales at the Australian Defence Force Academy, Canberra, ACT 2600, Australia

J. P. Escobedo-Diaz
e-mail: j.escobedo-diaz@unsw.edu.au

and the weapons created utilising it, it can be hard to distinguish fact from fiction regarding its performance characteristics. Despite this, there are numerous reports of the quality of Damascus steel being far higher than that of European steel in the early nineteenth century [2].

Genuine Damascus steel has a long and rather confusing history, which dates to the thirteenth century in India. The first time Europeans met Damascus steel, was in Persia, hence the name of Damascus steel. Similar process and material methodologies are known to have been in use across many different cultures. One of these was in Russia under the name of Bulat steel [3]. Another culture that embraced the process of using Damascus steel processes was traditional Japanese blade making, where the lower carbon steel, hocho-tetsu, was forged in with the higher carbon steel, tamahagane, in order to retain the edge hardness and retention of the tamahagane on the cutting edge, whilst also leveraging the shock absorption of the hocho-tetsu in the spine [4].

The original Damascus in India was produced via smelting iron which resulted in an inhomogeneous microstructure throughout the hypereutectoid steel [5]. It is commonly accepted that during the cooling phase, the damascene patterns are features of semi-uniform bands of cementite that formed parallel to the forging surface [6]. This is also known as carbide-banding phenomenon [2]. The patterns then emerged on the blades as the Bladesmith manipulated the blade plane to intercept that of the cementite bands and as such reveal the pattern so often associated with Damascus. In addition, some interesting performance characteristics emerged caused by the differing strength throughout the blade. The formation of these bands within genuine Damascus is still under investigation but is known to be directly related to the heat treatment process and the unique combination of impurities as a result of the manufacturing process [2].

Modern Damascus steel, or fire welded pattern steel, is primarily designed for the aesthetic appeal over performance, however, there is very limited research investigating the performance of this material under dynamic testing conditions or uniaxial stress. It is important to note that modern Damascus is different from genuine Damascus, the damascene pattern of the genuine version was a function of the microstructure, whereas the pattern of the modern version is a function of the difference between the fire welded alloys used to create it [7].

In this paper, we present our results of the characterization of modern Damascus steel, with particular interest in the response of the samples under quasi-static and dynamic loading conditions. These results include optical and electron microscopy imaging, hardness testing, and compression testing at different strain rates.

## Material and Experimental Methods

Two Damascus steels were used in this study, they were made out of 1095 and 15N20 steels. Two plates (50 mm wide, 150 mm long, and 10 mm thick) consist of

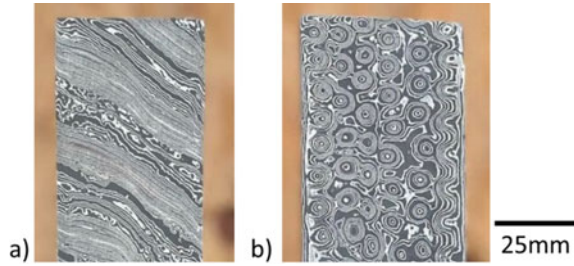**Fig. 1** Image of **a** Twist pattern sample; **b** Raindrop pattern sample



a)          b)          25mm

**Table 1** Chemical composition of the parent materials 1095 and 15N20

| Elements | Fe | C | S | P | Mn | Ni | Cr | Si |
|---|---|---|---|---|---|---|---|---|
| 1095 | 98.40 | 0.95 | 0.05 | 0.04 | 0.4 | 0.00 | 0.00 | 0.00 |
| 15N20 | 96.40 | 0.75 | 0.00 | 0.00 | 0.4 | 2.00 | 0.11 | 0.30 |

250 layers were used with different patterns: a twist pattern (Fig. 1a) and a raindrop pattern (Fig. 1b). Table 1 lists the chemical compositions of the materials.

The twist pattern material is made by fire welding the two steels together, drawing them out and then refolding them until the required layer count is obtained. Then, the material is forged into a square bar and twisted to a high degree. Once completed, the newly twisted bar is then reforged into flat bar stock, from which the sample acquired for these experiments was cut. The rain drop pattern follows a similar process to the twist pattern by stacking and refolding the dissimilar steels until the required layer count is obtained. Next, small holes were drilled in the steel and then the bar was reforged flat, allowing the layers to flow into the small gaps created by the drill.

These two different patterns were chosen primarily because the orientation of the layer boundaries will be significantly different. The orientation of the layer boundaries in reference to the loading axis will be approximately 90° for the rain drop pattern, while the twist pattern will be approximately 45°. Figure 1 shows the face of the material that was compressed.

Once the samples were rough forged, with the internal folds and twists completed for each pattern, the material was then finish forged into a flat bar with dimensions approximately 120 mm × 60 mm × 12 mm. This flat bar was then ground into the final dimensions of the sample, 100 mm × 50 mm × 10 mm, plus or minus 1.5 mm. The samples were then rough polished using a belt grinder using a 600-grit belt and etched with Ferric Chloride in order to show the pattern and contrast between the two steels. This etching will be polished off during experimentation, however, some samples will be re-etched for imaging and microscopy purposes, after further polishing and mounting.

The hardness testing of the material was completed for the as-received material. This testing was done on the Shimadzu Micro Hardness Tester HMV-G21 which enabled the individual testing of the different materials within the Damascus samples. The procedure for mounting and polishing resulted in a surface finish that visually

**Fig. 2** Optical image of
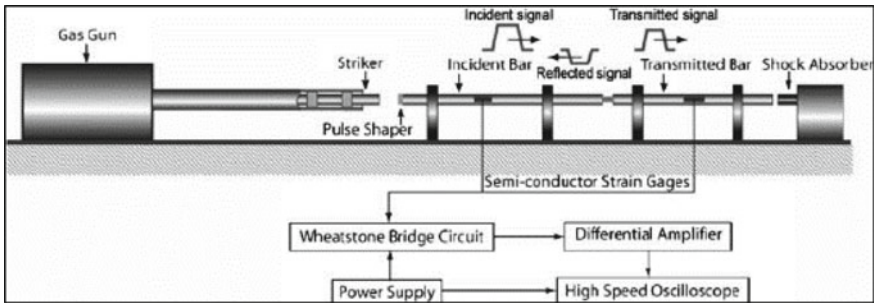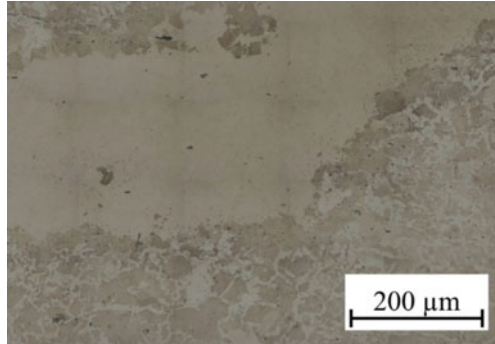Damascus sample showing
distinction between layers





**Fig. 3** Split-Hopkinson pressure bar set-up [8]

displayed the pattern of the Damascus, and a Nital etching solution was used to
expose the grain boundaries. This resulted in a surface finish distinct enough to
accurately test both materials separately (Fig. 2). Hardness tests were conducted in
several different positions within each individual layer in order to verify the results
and increase experimental accuracy.

Quasi-static compression testing was conducted on a Shimadzu Universal Testing
Machine, with a strain rate of $10^{-3}$/s. The operating parameters of the SHPB tests
(Fig. 3) were set such that strain rate of 1000–2000/s was imposed on each material.

Imaging has been conducted on conventional bright-field, differential interfer-
ence contrast on a Zeiss Axio Optical Microscope. Scanning electron and electron
backscatter microscopy were also conducted on the specimens.

## Results and Discussion

The hardness of the 1095 specimen was measured as 225 HV while the 15N20
material was measured to be 430 HV. The difference in hardness of the materials
was not expected given their similar chemical composition, specifically of carbon

content, which is of primary concern in regard to the hardness of steel. This difference in hardness of the materials could be caused by the alloying elements in the 15N20 material, being primarily nickel. It should also be noted that it is commonly known that both materials have a similar carbon content and as such, it is standard in the blacksmithing industry to treat 15N20 with the same process as basic high carbon knife making steels, 1095. It is then therefore safe to state that the annealing procedure followed in the production of the material has been optimised for 1095, rather than the more chemically complex 15N20.

The difference in hardness of the materials could mean that the initial deformation of the material will happen within the softer material, the 1095, and then transition into the 15N20 material. This could extend the time of the compression of the material and as such increase the spread of the load throughout the material. This also means that a majority of the damage will occur within the 1095 material, to a certain threshold, in which damage or deformation will occur in the 15N20 material.

The quasi-static stress–strain responses are shown in Fig. 4. Both materials, Raindrop and Twist pattern, display very similar response, with the Raindrop pattern sample having a slightly higher Youngs modulus. Compliance correction was completed on the Shimadzu Universal Testing Machine by running the quasi-static compression cycle with no sample present, in order to track the degree of movement of the machine under loading. This data was then zeroed in order to exclude the machine movement from the future testing. It was found that both materials have an approximate yield strength of 500–550 MPa and the strain hardening of the materials is also very similar.

The dynamic stress–strain responses are shown in Fig. 5. Once again, the response of the different pattern materials is very similar. Both twist and raindrop patterns display a yield strength in the 1100–1200 MPa

A pulse shaper was not used in these experiments but it can be seen from the force equilibrium graph, Fig. 6, that though there is a marked oscillation in the elastic
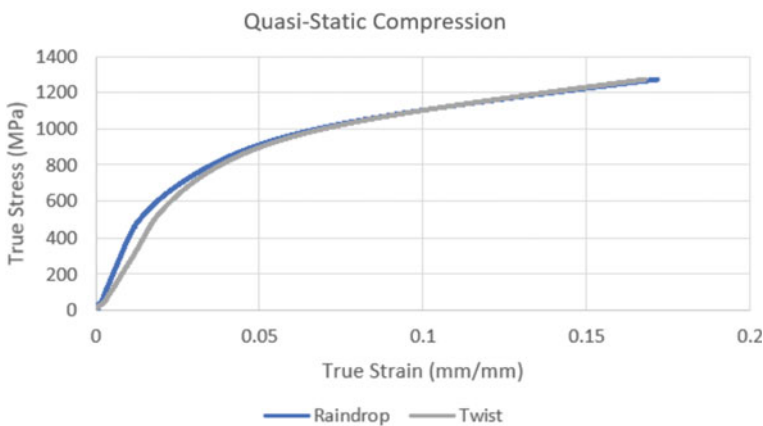


**Fig. 4** True stress–strain curves from the quasi-static testing of Damascus samples
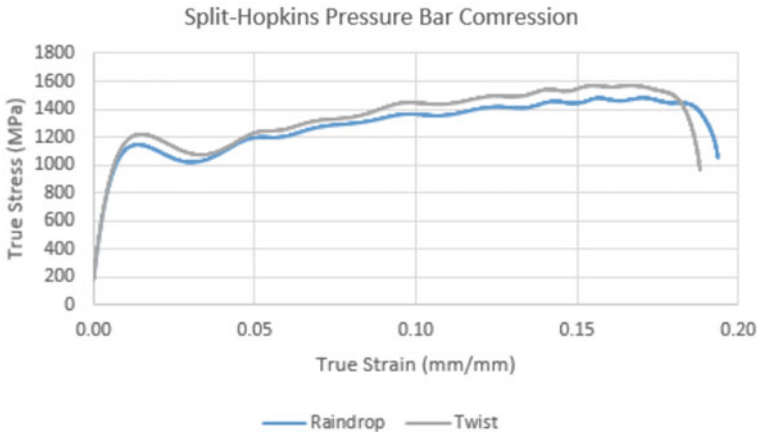
Split-Hopkins Pressure Bar Comression



**Fig. 5** True stress–strain compression curves from the dynamic deformation of Damascus samples

portion of the graph, the oscillations decrease in the plastic region. Furthermore, the front and rear force waves follow a similar gradient.

Optical and SEM images in Fig. 7 show that most defects and imperfections within the material occur in the 1095 layer of the samples. This might primarily occur in the production stage of the materials and it is a function of the high degree of deformation in this process. This could also be due to the difference in hardness of the two base materials, meaning that more of the deformation in the manufacturing process occurs in the softer material, thereby leaving the 15N20 with less deformation and as such a lower chance of inclusions or imperfections occurring. It should be noted that both materials show effects of porosity, signified by the small round imperfections in the
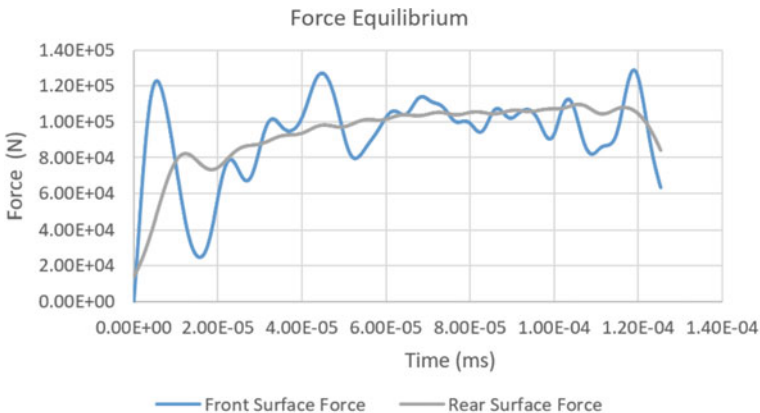
Force Equilibrium



**Fig. 6** Force equilibrium graph for SHPB compressive deformation of Damascus samples
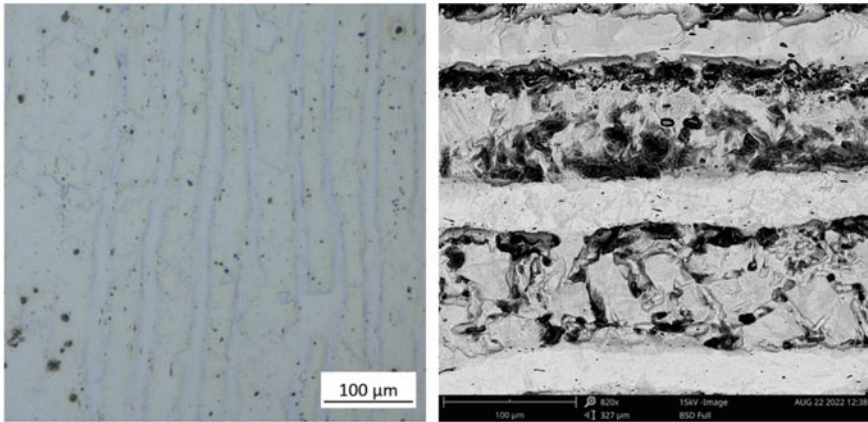
**Fig. 7** Images of a Damascus steel sample **a** Optical; **b** SEM

material, and this is a function of the as-received base material the Damascus pattern samples are made from, rather than that of the manufacturing process.

Figure 7 shows a clear and distinct layer boundary formed at the interface of the 1095 and 15N20 materials, with a clear difference in the microstructure of each material evident. Within the 1095 material, a relatively clear grain structure can be seen, with a relatively large size difference present. The chemical makeup of this material can be seen in Fig. 8, which shows an EDS overlay of carbon, iron, and nickel. No nickel is present the 1095 bands but has a relatively even distribution throughout.

Due to the difference in hardness of the two materials, there is a relief between them, in which the softer 1095 has been polished to beneath that of the 15N20.

It should also be noted that a majority of the visible imperfections within the materials appear within the 1095 material, Fig. 7. Once again this could be due to the manufacturing process, where more of the deformation occurs within this material, and as such it increases its likelihood of inclusion and other imperfections within the material. This could lead to failure occurring within this material first when under higher loading.

The composition of the 15N20 material is more difficult to understand, as its microstructure wasn't visible under bright-field microscope and is only partially evident under SEM. The distinction between microstructure within the material can be seen by the slight variation within the colour of the material. The heavier materials, primarily nickel and manganese are shown as lighter whilst the lighter elements are darker within Fig. 8.
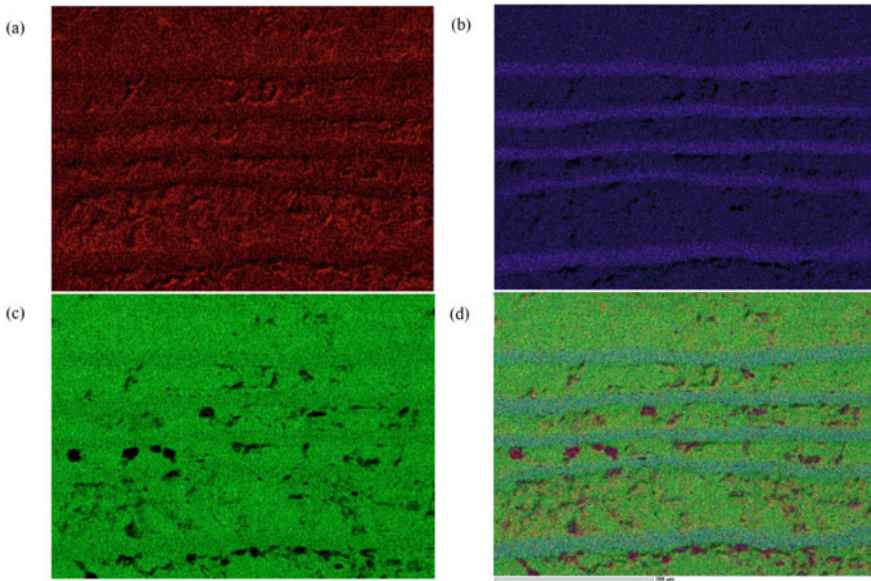
**Fig. 8** EDS image of 10 **a** Carbon; **b** Nickel; **c** Iron; **d** element overlay

## Conclusions

Through imaging, compression, and hardness testing, the characterisation of a couple of Damascus steel materials has been conducted. It has been shown that there is a difference in the hardness of the materials, likely caused by the alloying elements in the 15N20 material, paired with the optimisation of annealing for the 1095 material. The difference in hardness also results in a majority of manufacturing deformation occurring within the 1095 material, which also leads to a higher percentage of imperfections occurring within this material.

The grain size of the materials appears to be relatively similar, with the structure of the 15N20 being more consistent, while the 1095 structure appears to have a larger variety, possibly caused by the higher level of manufacturing deformation.

The stress–strain response in quasi-static and SHPB experiments show that there are only slight differences in the response of the material as a function of the pattern of the sample, with the twist pattern returning a very slightly higher yield strength than the raindrop pattern under dynamic loading.

# References

1. Verhoeven J, Pendray A, Gibson E (1996) Wootz Damascus steel blades. Mater Charact 37(1):9–22
2. Sukhanov D, Arkhangel'skii L (2016) Damascus steel microstructure. Metallurgist 59(9–10):818–822
3. Verhoeven J (2002) Genuine Damascus steel: a type of banded microstructure in hypereutectoid steels. Steel Res 73(8):356–365
4. Peterson D, Baker H, Verhoeven J (1990) Damascus steel, characterization of one Damascus steel sword. Mater Charact 24(4):355–374
5. Verhoeven J, Pendray A (2001) Origin of the Damask pattern in Damascus steel blades. Mater Charact 47(5):423–424
6. Pendray A, Dauksch W (1998) The key role of impurities in ancient Damascus steel blades. JOM 50(9):58–64
7. Wadsworth J, Sherby O (1980) On the Bulat—Damascus steels revisited. Prog Mater Sci 25(1):35–68
8. Sunny G, Yuan F, Prakash V, Lewandowski J (2009) Design of inserts for split-Hopkinson pressure bar testing of low strain-to-failure materials. Exp Mech 49(4):479